ADAPTIVE TEMPERATURE CONTROL ALGORITHM FOR THE EXTRUDER BASED ON RBFNN AND NUSSBAUM-TYPE FUNCTION

Bo XU[1]*, Luyao YUAN[2], Lingyu YIN[3]

As the core equipment in rubber production, the temperature control accuracy of the rubber extruder affects the final product quality. However, the temperature change of the material in the rubber extruder is complex and nonlinear, and the modelling of the temperature change process is difficult. It is difficult to accurately track and control the temperature using the traditional proportional integral differential algorithm (PID). This paper investigates a temperature trajectory tracking algorithm for rubber extruder systems. An algorithm based on RBF neural network (RBFNN) is proposed for the extruder to track the temperature curve. The RBFNN is used to fit the model of the plant automatically, and the Nussbaum-type function is used to solve the problem of the unknown direction of the control variable. Finally, the stability of the algorithm is demonstrated by the Lyapunov stability analysis. The proposed algorithm has strong robustness compared to conventional algorithms and does not need modelling and parameter adjustment. The effectiveness and superiority of the proposed control algorithm are proven by the simulation results. If the algorithm is successfully applied to actual injection molding machine systems, it will greatly shorten the adjustment time of printing machine parameters, reduce the difficulty of adjustment, and increase the robustness of the equipment.

Keywords: Extruder; Nussbaum-type function; Back-stepping; RBFNN; Adaptive control

1. Introduction

In the field of rubber and plastic product manufacturing, extruders are key pieces of equipment, playing a central role in the extrusion and shaping process. The temperature of the extruder is one of the core process parameters. Fluctuations in temperature can cause changes in the melt viscosity of the granulate, which in turn affects the extrusion flow rate and die pressure.[1] Precise temperature control is an essential part of precision extrusion molding. If the temperature parameters are not well-regulated, it can lead to large steady-state errors and overshoots, resulting in temperatures that are too high or too low. [2] This can affect the

[1] Dept. of Electrical and Mechanical, Beijing Information Science and Technology, Beijing, China, e-mail: xubo821130@bistu.edu.cn
[2] Dept. of Electrical and Mechanical, Beijing Information Science and Technology, Beijing, China, e-mail: 41120703@qq.com
[3] China Software Testing Center, Beijing, China, e-mail: yinlingyu@cstc.org.cn

material's shrinkage rate, thermal degradation, and the melting and plasticization effect. A typical heating tube is divided into three different temperature zones: the feed zone, transition zone, and melting zone (see Fig. 1). Extruders have a large thermal inertia coefficient, and traditional PID control methods result in large overshoots, wide temperature fluctuations, slow adjustment speeds, long adjustment times, and poor parameter robustness. They are easily affected by environmental factors, with the same PID parameters performing differently in winter and summer. Therefore, the parameter adjustment for injection molding machines requires a high level of technical expertise from operators. Finding a temperature control algorithm for injection molding machines that can achieve automatic parameter adjustment and has strong robustness is key to solve the above issues [3,4]:

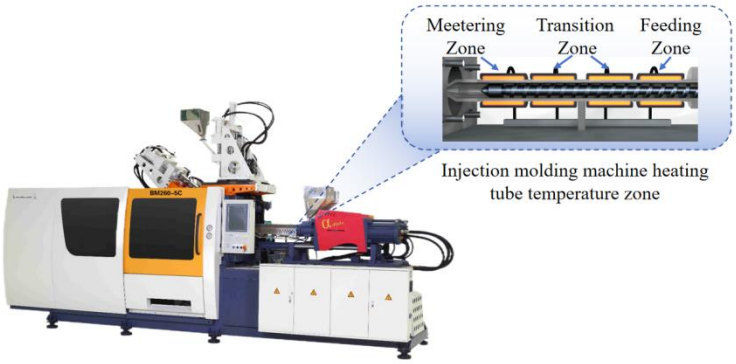

Fig.1 Structural drawing of feeding heating pipe

2. Problem statement

To address the above issues, numerous scholars have conducted research in this field. The earliest efforts include the digital PID introduced by Dormeier [5] combined with a multi-mode control algorithm. Segmented PID reduces the difficulty of PID parameter adjustment by segmenting the controlled object. Designing multiple sets of PID parameters to meet the control requirements of rapid heating at the initial stage and small overshoot after approaching stability. Different PID parameters are used for control according to different stages of control requirements. Representative efforts include designing various multi-modal strategies to control pipeline temperatures. Although this solution is more targeted and enhances control performance, making it easier to adjust each set of PID parameters, it increases the number of PID parameters, thereby increasing the workload for PID parameter tuning. Moreover, the switching of parameters may lead to instability in the injection molding machine system. [6]

In the late 1970s, adaptive control algorithms combining artificial intelligence technology became a research hotspot. Control algorithms such as

fuzzy control, neural networks, and iterative learning are applied to the local approximation of controlled systems to achieve precise model control. Representative work includes Chen et al. [7] developing a fuzzy adaptive control strategy system with multiple linear models for extruders, improving control accuracy. Yao et al. [8] used optimal time control to solve the problem of initial temperature rise in machine pipelines. Predictive control and feedforward iterative learning control [9] were used to achieve temperature control during the transition phase of injection molding machine pipelines. The article [10] designed a fuzzy controller to eliminate the coupling between melting temperature and pressure during the extrusion process. Wei proposed a variable structure temperature control strategy for injection molding machines based on iterative learning, improving the dynamic control accuracy of the injection molding machine and reducing the difficulty of parameter adjustment. [11] Meanwhile, they also tried the cerebellar model articulation controller (CMAC) neural network method to achieve control of the injection molding machine. [12] Aiming at the coupling and nonlinear problems of the temperature control system of the injection molding machine barrel, Hu et al. combined the advantages of fuzzy algorithm and neural network algorithm to design a fuzzy neural network decoupling compensator, improving the accuracy and stability of the temperature control of the injection molding machine barrel. [13] Among these intelligent algorithms, temperature control algorithms based on neural networks are the most widely used and relatively effective.[14] Artificial neural networks are an information processing model that simulates the structure and function of human brain neurons. It has strong nonlinearity and adaptability. [15] In the field of control, it is often used for nonlinear modeling and function approximation. The application of neural networks greatly simplifies the difficulty of parameter adjustment in traditional control algorithms and improves control performance at the same time. Representative work is Zhu et al. [16] combining traditional PID controllers with radial basis function (RBF) neural networks to control melt temperature and achieve PID parameter adjustment. Li et al. [17] established a neural network basic structure and model for temperature control of injection molding machine barrels based on the SPIDNN (single-output attribute integration derivative neural network) algorithm, improving control accuracy. Most of the above methods are based on traditional PID algorithm control methods, which roughly adjust PID parameters first, and then use neural network methods for local compensation. The biggest disadvantage of these methods is that they still need to establish a system based on PID parameters, which cannot avoid manual PID parameter adjustment.

To address the above issues, this paper proposes a neural network automatic parameter adjustment method based on a large-scale neural network. The main feature of this method is that it does not require basic modeling or PID parameter adjustment. The system realizes the control of the controlled object through automatic fitting by the neural network algorithm, which greatly reduces the dependence on the control system parameters. Compared with traditional neural

network modeling methods, this algorithm also introduces the Nussbaum function, cleverly avoiding the problem of singular points in neural network fitting when the parameters to be fitted are in the denominator, and non-convergence of the fitting results. [18,19] Combined with adaptive control, it further improves the anti-interference ability of the system.

3. Research and research methods

3.1 research methods

To address the complexities and poor robustness in adjusting system parameters for injection molding machines, a controller design was proposed. The method includes the following:

Firstly, establishing a mathematical model of the injection molding machine's heating pipe system, abstracting the injection molding machine as a typical second-order system. Then, an adaptive neural network is used to approximate the model of the injection molding machine, while a Nussbaum-type approach is employed to approximate the coefficient of the control variable u. The introduction of the Nussbaum-type resolves issues where singular points exist in the denominator of the control input coefficient. Due to the fact that actual injection molding machine systems are not open for research, a semi-physical model test bench is constructed for convenience in obtaining data from the model of the controlled object. Finally, through experiments, the functionality of the controller is verified.

3.2 Preliminaries

3.2.1 Problem formulation

Assuming that a single temperature zone is a second-order system, the state space equations are shown by Eq. (1):

$$\begin{cases} \dot{x}_1 = x_2 \\ \dot{x}_2 = f\,(x) + \varphi(x)u + d(t)\,, \\ y = x_1 \end{cases} \tag{1}$$

where $x = [x_1, x_2]^T \in R^n$, x denotes a column vector. $u \in R$ and $y \in R$, u and R denote the input and output. $f\,(x)$ and $\varphi\,(x)$ denote unknown smoothing functions that satisfy the local Lipschitz condition, the initial value of $\varphi\,(x)$ is not equal to zero and $\varphi\,(x)$ is bounded. $d\,(t)$denotes the external disturbance induced by other temperature zones and bounded by a known constant, $|d\,(t)\,| \leq D$. The goal is to force the output y to follow an ideal trajectory.

3.2.2 RBFNN approximation

The Radial Basis Function Neural Network (RBFNN) serves as a powerful tool in approximating the elusive continuous system function. The formulation of the RBFNN is articulated as follows:

$$\hat{f}(\theta|W) = W^T S(\theta), \tag{2}$$

where $\theta \in R^m$, θ denotes the input vector, $\hat{f}(\theta|W)$ represents the estimation of the structural function $f\ (x)$ in the transfer function, n > 1 denotes the RBFNN node quantity, W $\in$ Rn denotes the weight vector, and S(θ) = [s1(θ), s2(θ)... sn(θ)]T denotes the basis function vector. Herein, the Gaussian function is selected as the basis function vector:

$$S_i(\theta) = exp\left[\frac{-(\theta - \mu_i)^T(\theta - \mu_i)}{2\eta_i{}^2}\right], \quad (3)$$

Where$\mu_i = [\mu_1, \mu_2, \dots\dots,, \mu_n]^T$, μ_i represents the width of the Gaussian function associated with the respective receptive field. RBFNN can approximate any continuous function on a compact set $\Omega_x \subset R_q$with an arbitrary precision of $f\ (\theta|W) = W^{*T}S\ (\theta) + \varepsilon$ and$\forall\theta \in \Omega_\theta$ where W^* denotes the ideal constant weight, and ε denotes the approximation error.

Assumption 1: There is an unchanged weight W^* that satisfies $|\varepsilon| \leq \varepsilon^*$,

$$W^* \triangleq \arg\min_{w\in R^l}\left\{\sup_{z\in\Omega_z}|f(w) - W^Ts(\theta)|\right\}. \quad (4)$$

$\varepsilon^* > 0$, for all.

Parameter W^* is chosen according to the controlled object's features to acquire the minimal value.

Assumption 2: The weight vector W and the activation function S are upper bounds, $||W|| \leq W_M$ and $||S|| \leq S_M$.Parameters W_M and S_M are unknown positive constants.

3.2.3 Nussbaum-type function gain

In 1983, Rogers Nussbaum proposed Nussbaum-type functional gain to solve the problem of unknown high-frequency acquire symbol of virtual controller [20]. This virtual controller is used to solve the calming problem of dynamically designing parameters to solve the system in the parameter adaptive feedback control system. The difficulty is how to find the reciprocal of the control rate u 's coefficient. If the neural network method is still used for identification, the $\varphi(x)$ symbol (As shown in Equation 1) will change from negative to positive, which will appear to be 0, causing the system control to diverge. After adopting the Nussbaum-type function method [21], the role of the Nussbaum-type function in the calm control system is to switch symbols and change the amplitude, driving the system state to constantly "swing", so that the state can swing up and down when the system state is close to 0, the system state and Nussbaum-type function derivative will correspond to 0. This turns a problem of discerning division into a problem of multiplication. This eliminates the need to know whether the control direction of the system is positive or negative. Divergence is avoided.

The Nussbaum-type function has been widely applied to industrial control, military industry, and many other fields.

In this paper, the Nussbaum-type function solves the problem of the unknown direction of control variable coefficients.

The following definitions and lemmas are provided here:

Definition 1: The Nussbaum-type function has the following properties:

$$\lim_{s\to\infty} sup\frac{1}{s}\int_0^s N(\chi)d\chi = +\infty, \tag{5}$$

$$W^* \triangleq \arg\min_{w\in R^l}\left\{\sup_{z\in\Omega_z}|f(w) - W^T s(\theta)|\right\}. \tag{6}$$

The Nussbaum-type function is selected as follows:

$$N(\chi) = \chi^2 cos(\chi). \tag{7}$$

Lemma 1: $V(t)$ and $\chi(t)$ are defined at the interval $t \in [0, t_f]$, where $V(t) \geq 0$ if the following inequality holds:

$$V(t) \leq c_0 + e^{-c_1 t}\int_0^t (g(\tau)N(\chi) + 1)\dot{\chi}e^{-c_1\tau}d\tau. \tag{8}$$

For smooth functions $V(t) \geq 0$, $g(\tau)$ is defined at [0, t_f], $\chi(t)$ is a smooth Nussbaum-type function, c_0 is an appropriate constant, $c_1 > 0$, $V(t)$, $\chi(t)$, and $\int_0^t (g(\tau)N(\chi) + 1)$ must be bounded on the interval $t \in [0, t_f]$. A Nussbaum-type function will be used to estimate the control direction in future work.

Lemma 2:（Barbalat Lemma ）For function $\varepsilon(\tau)$: $R^+ \to R$, if $\varepsilon(\tau)$ is consistently continuous and $\lim_{t\to\infty}\int_0^t \varepsilon(\tau)\,d\tau$ exists and is bounded, then: $\lim_{t\to\infty}\varepsilon(\tau) = 0$

3.3 Controller design and stability analysis

3.3.1 Controller design

An adaptive temperature controller of the extruder based on RBFNN and Nussbaum-type function is designed in this section. The basic control block diagram is shown in Fig. 2.

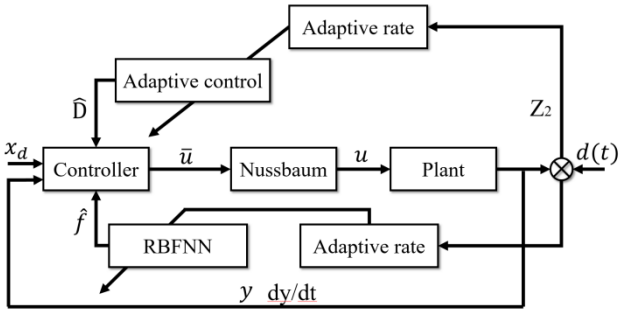

Fig.2 The structure diagram of the control system

Where in the subject is an extruder barrel of unknown structure, and the model of the subject is described in Equation 1. Since the system structure parameter $f(x)$, the control variable coefficient $\varphi(x)$, and the perturbation $d(t)$ of the system are unknown, the control rate u of the system cannot be designed. To

solve the problem, adaptive neural networks are used to identify the structural parameters $f\ (x)$ of the system. The Nussbaum-type function method is adopted to identify the 1/ $\varphi(x)$. Finally, the adaptive neural network is used to compensate for the disturbance variable $d(t)$, and the method is simple and has strong engineering application value.

The design process is divided into three steps. First, the back-stepping method is used to design the controller. Second, the Nussbaum-type function is introduced to design the controller. Lastly, the RBFNN is introduced to calculate the adaptive system rate.

Step 1: Design the controller using the backstepping method.

parameter x_d is defined as the tracking trajectory of the target and z_i is the tracking error. Then:

parameter $\mathrm{x_d}$ is defined as the tracking trajectory of the target and $\mathrm{z_i}$ is the tracking error. Then:

$$z_1 = x_1 - x_{1d}. \tag{9}$$

Define the system state error:

$$z_2 = x_2 - x_{2d}. \tag{10}$$

Design a controller targeting the error and construct a Lyapunov equation as follows:

$$V_1 = \frac{1}{2} z_1^2. \tag{11}$$

Then:

$$\dot{V}_1 = z_1 * \dot{z}_1. \tag{12}$$

From equation (9), we obtain:

$$\dot{z}_1 = \dot{x}_1 - \dot{x}_{1d}. \tag{13}$$

Based on the controlled object model given by equation (1), where ($\dot{x}_1 = x_2$), equation (12) can be rewritten as:

$$\dot{V}_1 = z_1(x_2 - \dot{x}_{1d}). \tag{14}$$

Designing the controller$x_{2d}$to follow$x_2(t)$， in order to ensure system stability, we have:

$$x_{2d} = -kz_1 + \dot{x}_{1d}. \tag{15}$$

Combining equation (15) with equation (10) and substituting into equation (14), we get：

$$\dot{V}_1 = z_1(-kz_1 + \dot{x}_{1d} - \dot{x}_{1d} + z_2) = -k_1 z_1^2 + z_1 z_2. \tag{16}$$

Construct the second Lyapunov equation:

$$V_2 = V_1 + \frac{1}{2} z_2^2. \tag{17}$$

Then:

$$\dot{V}_2 = \dot{V}_1 + z_2 \dot{z}_2 = -k_1 z_1^2 + z_1 z_2 + z_2 \dot{z}_2 = -k_1 z_1^2 + z_2(z_1 + \dot{z}_2). \tag{18}$$

From equation (10), we obtain:

$$\dot{z}_2 = \dot{x}_2 - \dot{x}_{2d} \tag{19}$$

.

By substituting the controlled object model given by equation (1) into equations (18) and (19), the control rate can be obtained, that is:

$$\dot{V}_2 = -k_1 z_1^2 + z_2(z_1 + f\ (x) + \varphi(x)u + d(t) - \dot{x}_{2d}) \tag{20}$$

Based on equation (20), the control law can be designed as shown in equation (21).

$$u = \frac{1}{\varphi(x)}(-f(x) + \dot{x}_{2d} - d(t)) \tag{21}$$

.

However, in practical control, there are three evident issues. Firstly, to achieve model-free temperature control of the injection molding machine, the model of the injection molding machine is unknown. Secondly, the disturbances during the production process are bounded, but the disturbance model is also unknown. Lastly, the coefficient function of the controller is unknown and is in the denominator. If a simple neural network fitting approach is used, the entire control system will diverge and become uncontrollable when passing through zero. This paper adopts the following methods to solve the above problems:

For the unknown issues, an adaptive neural network method is employed for fitting. The system model and disturbance model are automatically approximated through the neural network. For the problem of unknown magnitude and direction of the control rate coefficient function, a Nussbuam-type function is used for fitting. Finally, this forms the overall control rate function. The specific implementation steps are as follows:

Step 2: To achieve automatic identification of the model, neural network control is introduced.

The RBFFNN is used to fit the unknown items in the controlled object. The ideal output of the bit fitting error network is shown by Eq. (22):

$$f(x) = W^{*T}s(x) + \varepsilon_f. \tag{22}$$

Parameter vector μ_i of $s\ (x)$ is selected, as shown in equation (3). Parameter W^* is the ideal network weight, $\widehat{W}$ is the estimated weight of the network, ε_f is the network approximation error (bounded), and $r = [z_1, \dot{z}_1]$ is the network input. The actual network output is shown in Eq. (23):

$$\hat{f}(x) = \widehat{W}^T s(x), \tag{23}$$

where $\widetilde{\mathrm{W}}$ is the difference between the estimated weight value $\widehat{\mathrm{W}}$ and the ideal weight value W^*:

$$\widetilde{W} = \widehat{W} - W^*. \tag{24}$$

After fitting with neural networks, we choose the Lyapunov function again, and formula (22) is rewritten as:

$$V_2 = V_1 + \frac{1}{2}z_2^2 + \frac{1}{2r_1}\widetilde{W}^T\widetilde{W} + \frac{1}{2r_2}\widetilde{D}^T\widetilde{D}, \tag{25}$$

$$\widetilde{D} = d(t) - \widehat{D} + \varepsilon_d \tag{26}$$

As mentioned above, $|d(t)| \leq D$ represents the bounded disturbance, which comes from the adjacent temperature zone. Parameter D represents the upper bound of the disturbance, $\widehat{D}$ represents an estimate of the disturbance, $\widetilde{D}$ represents the difference between the existing system and the estimated value, ε_{d} represents the estimation error, ε_d is a bounded-function, and $||\varepsilon_d|| \leq \varepsilon_D$. Parameter $\dot{V}_2$ is shown in Eq. (27).

$$\dot{V}_2 = \dot{V}_1 + z_2\dot{z}_2 + \frac{1}{r_1}\widetilde{W}^T\dot{\widehat{W}} + \frac{1}{r_2}\widetilde{D}^T\dot{\widehat{D}} \tag{27}$$

Combining equation (1), equation (27) can be transformed into equation (27).

$$\dot{V}_2 = \dot{V}_1 + z_2(f(x) + \varphi(x)u + d(t) - \dot{x}_{2d}) + \frac{1}{r_1}\widetilde{W}^T\dot{\widehat{W}} + \frac{1}{r_2}\widetilde{D}^T\dot{\widehat{D}} \tag{28}$$

Step 3: The nussbaum function is used to eliminate the function in the denominator of the control law.

The Nussbaum-type function, shown in Eq. (29), is used to design the controller. The Nussbaum-type function is commonly used to solve the problem of the unknown direction of the controller's coefficients.

$$\begin{cases} u = N(\chi)\bar{u} \\ \bar{u} = k_2 z_2 + \hat{f}(x) - \dot{x}_{2d} + \widehat{D} - z_1 \\ \dot{\chi} = \bar{u} z_2 \end{cases} \tag{29}$$

where $N(\chi) = \chi^2 cos(\chi)$.

Substitute (29) into equation (28) for ($z_2\varphi(x)u$) to simplify and obtain equation (30).

$$\dot{V}_2 = \dot{V}_1 + \varphi(\tau)N(\chi)\dot{\chi} + z_2(f(\theta) + d(t) - \dot{x}_{2d}) + \frac{1}{r_1}\widetilde{W}^T\dot{\widehat{W}} + \frac{1}{r_2}\widetilde{D}^T\dot{\widehat{D}} \tag{30}$$

Perform a mathematical operation here, which involves adding or subtracting an $\dot{\chi}$.

$$\dot{V}_2 = \dot{V}_1 + (\varphi(\tau)N(\chi) + 1)\dot{\chi} - \dot{\chi} + z_2(f(\theta) + d(t) - \dot{x}_{2d}) + \frac{1}{r_1}\widetilde{W}^T\dot{\widehat{W}} + \frac{1}{r_2}\widetilde{D}^T\dot{\widehat{D}} \tag{31}$$

Substitute ($\dot{\chi} = \bar{u}z_2$) into equation (31):

$$\dot{V}_2 = \dot{V}_1 + (\varphi(\tau)N(\chi) + 1)\dot{\chi} + z_2(f(x) + d(t) - \dot{x}_{2d} - \bar{u}) \tag{32}$$

Eq. (32) can be obtained by further simplification:

$$\dot{V}_2 = \dot{V}_1 + (\varphi(\tau)N(\chi) + 1)\dot{\chi} - k_2 z_2^2 + z_2\left(f(\theta) - \hat{f}(\theta) + d(t) - \widehat{D} + z_1\right) + \frac{1}{r_1}\widetilde{W}^T\dot{\widehat{W}} + \frac{1}{r_2}\widetilde{D}^T\dot{\widehat{D}}. \tag{33}$$

By substituting Eq. (16) into Eq. (33), Eq. (34) can be obtained:

$$\dot{V}_2 = -k_1 z_1^2 - k_2 z_2^2 + (\varphi(\tau)N(\chi) + 1)\dot{\chi} + z_2\left(f(\theta) - \hat{f}(\theta) + d(t) - \widehat{D}\right) + \frac{1}{r_1}\widetilde{W}^T\dot{\widehat{W}} + \frac{1}{r_2}\widetilde{D}^T\dot{\widehat{D}}, \tag{34}$$

Step 4: The RBFNN is used to fit the controlled object mode $f(x)$and the disturbance signal $d(t)$. Eqs. (22) and (23) can be combined to obtain Eq. (35):

$$\tilde{f}(x) = f(x) - \hat{f}(x) + \varepsilon_f = -\widetilde{W}^T s(x) + \varepsilon_f. \tag{35}$$

The difference between the actual value and the estimated value is shown in Eq. (36):

$$\widetilde{D} = d(t) - \widehat{D} + \varepsilon_d, \tag{36}$$

Eq. (37) is obtained by simplifying Eq. (31) and combining it with Eqs. (35) and (36):

$$\begin{aligned}\dot{V}_2 = -k_1 z_1^2 - k_2 z_2^2 + (\varphi(\tau)N(\chi) + 1)\dot{\chi} + z_2\left(-\widetilde{W}^T s(\theta) + \varepsilon_f - \widetilde{D} + \varepsilon_d\right) \\ + \frac{1}{r_1}\widetilde{W}^T\dot{\widehat{W}} + \frac{1}{r_2}\widetilde{D}^T\dot{\widehat{D}}.\end{aligned} \tag{37}$$

Eq. (38) is obtained by further simplifying Eq. (37):

$$\begin{aligned}\dot{V}_2 = -k_1 z_1^2 - k_2 z_2^2 + (\varphi(\tau)N(\chi) + 1)\dot{\chi} \\ +\widetilde{W}^T\left((-z_2 s(\theta) + \frac{1}{r_1}\dot{\widehat{W}}) + \widetilde{D}^T(-z_2 + \frac{1}{r_2}\dot{\widehat{D}})\right) + z_2\varepsilon_f + z_2\varepsilon_d,\end{aligned} \tag{38}$$

The adaptive rate is shown in Eqs. (39) and (40):

$$\dot{\widehat{W}} = r_1 z_2 s(\theta) - \frac{\sigma}{2}\widehat{W}, \tag{39}$$

$$\dot{\widehat{D}} = r_2 z_2 - \frac{\rho}{2}\widehat{D}. \tag{40}$$

3.3.2 Stability analysis

Parameter $\dot{V}_2$ is obtained by substituting Eqs. (40) and (39) into Eq. (38):

$$\begin{aligned}\dot{V}_2 = -k_1 z_1^2 - k_2 z_2^2 + (\varphi(\tau)N(\chi) + 1)\dot{\chi} - \frac{\sigma}{2r_1}\widetilde{W}^T\widehat{W} \\ -\frac{\rho}{2r_2}\widetilde{D}^T\widehat{D} + z_2\varepsilon_f + z_2\varepsilon_d.\end{aligned} \tag{41}$$

Eq. (41) can be further simplified:

$$2\widetilde{W}^T\widehat{W} = ||\widetilde{W}||^2 + ||\widehat{W}||^2 - ||W^*||^2 \geq ||\widetilde{W}||^2 - ||W^*||^2, \tag{42}$$

The same principle leads to Eq. (43).

$$2\widetilde{D}^T\widehat{D} \geq ||\widetilde{D}||^2 - ||D^*||^2 \tag{43}$$

Let $\varepsilon_H=\varepsilon_f+\varepsilon_d$ and scale $\dot{V}_2$ to get Eq. (44):

$$\begin{aligned}\dot{V}_2 \leq -k_1 z_1^2 - k_2 z_2^2 - \frac{\sigma}{2r_1}\left(\left|\left|\widetilde{W}\right|\right|^2 - \left|\left|W^*\right|\right|^2\right) \\ -\frac{\rho}{2r_2}\left(||\widetilde{D}||^2 - ||D^*||^2\right) + z_2\varepsilon_H + (\varphi(\tau)N(\chi).+1)\dot{\chi}\end{aligned} \tag{44}$$

Scale transformation according to Yang inequality:

$$\begin{aligned}\dot{V}_2 \leq -k_1 z_1^2 - k_2 z_2^2 - \frac{\sigma}{2r_1}\widetilde{W}^T\widetilde{W} - \frac{\rho}{2r_2}\widetilde{D}^T\widetilde{D} + z_2^2 + \frac{\varepsilon_H^2}{4} \\ +(\varphi(\tau)N(\chi) + 1)\dot{\chi} + \frac{\sigma||W^*||^2}{2r_1} + \frac{\rho||D^*||^2}{2r_2}.\end{aligned} \tag{45}$$

Select $k_1 \geq \frac{\gamma}{2}, k_2 - 1 \geq \frac{\gamma}{2}, \sigma \geq \gamma, \sigma \geq \gamma, \rho \geq \gamma$, where γ is a positive number. Let $\delta = \frac{||W^*||^2}{2r_1} + \frac{||D^*||^2}{2r_2} + \frac{\varepsilon_H^2}{4}$, perform scale transformation on Eq. (45) to obtain the following:

$$\dot{V}_2 \leq -\gamma \frac{z_1^2}{2} - \gamma \frac{z_2^2}{2} - \frac{\gamma}{2}\widetilde{W}^T\widetilde{W} - \frac{\gamma}{2}\widetilde{D}^T\widetilde{D} + (\varphi(\tau)N(\chi) + 1)\dot{\chi} + \delta, \tag{46}$$

$$\dot{V}_2 \leq -\gamma V_2 + (\varphi(\tau)N(\chi) + 1)\dot{\chi} + \delta. \tag{47}$$

Multiply both sides of the equation by $e^{\gamma t}$ and integrate both sides of Eq. (47) to obtain Eq. (50):

$$\dot{V}_2 e^{\gamma t} + \gamma V_2 e^{\gamma t} \leq (\varphi(\tau)N(\chi) + 1)\dot{\chi} e^{\gamma t} + \delta e^{\gamma t}, \tag{48}$$

$$\frac{d(V_2 e^{\gamma t})}{dt} \leq (\varphi(\tau)N(\chi) + 1)\dot{\chi} e^{\gamma t} + \delta e^{\gamma t}, \tag{49}$$

$$0 \leq V_2(t) \leq V_2(0)e^{-\gamma t} + e^{-\gamma t}\int_0^t (\varphi(\tau)N(\chi) + 1)\dot{\chi}\, e^{\gamma t} d\omega + \frac{\delta}{\gamma}. \tag{50}$$

According to the following lemma 1, it can be obtained that $V_2(t)$,$(\varphi(x)N(\chi) + 1)\dot{\chi}$,$\dot{\chi}$,$z_1$,$z_2$, $\widehat{W}$,$\widehat{D}$, are bound in a finite time. According to lemma 2, $\lim_{t\to\infty} V_2(t) = 0$, It can be seen from Equation (20),$V_1(t) = 0; V_1 = \frac{1}{2}z_1^2$, hence $\lim_{t\to\infty} z_1(t) = 0$can be obtained, meaning that the controller can track the set temperature curve ($z_1 = x_d - x_1$).

4. Simulation experiment verification of extruder temperature zone control

4.1 Construction of the simulation test bench and model identification

The control system of the extruder is a closed system with a control algorithm that is impossible to change and embed. Therefore, according to the characteristics of the extruder's zonal heating, an abstract simulation experiment platform is developed to understand the control characteristics of the extruder by researching and modeling the experiment platform. The model is established to understand the control characteristics of the extruder.

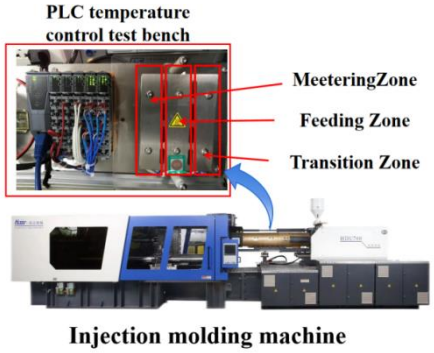

Fig.3 The extruder temperature control test bench

As shown in Fig. 3, the experimental platform is divided into three temperature zones to simulate the extruder system: the feeding zone, the transition zone, and the metering zone. The PLC controller independently controls the temperature of each zone. The temperature zone is heated by the heating rod (the input voltage of the heating rod is 24 V, and the power is 30 W). The PLC controls the temperature of the heating rod by controlling the switch of the solid-state voltage regulator (SSVR). Each zone has three temperature sampling points (feedback via type K thermocouples). Once the average value is calculated, it is used to estimate the actual temperature of this temperature zone (Fig. 4). The specific composition and parameters of the test bench are shown in Table 1.

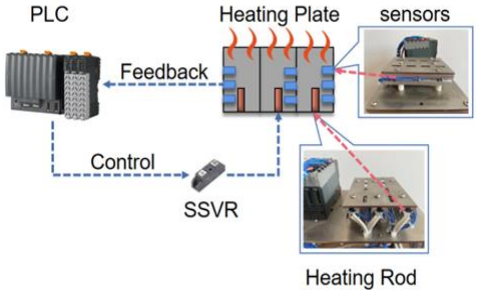

Fig.4. The layout of the heating rod and test bench sensor

Table 1

Test bench configuration

No	Module model	Device capabilities	Numbers
1	B&R X20CP1584	CPU	1
2	B&R X20BC0083	Communication module	1
3	B&R X20DO4322	Digital output and PWM control	1
4	B&R X20AT6402	Temperature feedback	1
5	SSVR	PWM control	1
6	Heating rod	Heating	3
7	Thermocouple	Temperature feedback	9

PLC controls the solid-state voltage regulator to heat the heating plate. The input power supply is 24 V, and the output temperature curve is recorded, as shown in Fig. 5. The temperature control system is modeled through the MATLAB system identification toolbox. The controlled system can be identified as a linear and a nonlinear system. Because the accuracy of the linear system is higher in the identification process, the system is identified as a transfer function.

$$G(s) = \frac{0.05718s + 0.001254}{s^2 + 0.06595s + 0.000222}, \tag{51}$$

The 24 V input excitation model is adopted and compared with the actual curve, as shown in Fig. 5. The results show that the model curve can coincide with the actual curve, and the coincidence rate of the frequency domain reaches 99.07%. The model's output can simulate the performance of the existing experimental system in time and frequency domains, providing a model for further algorithm simulation.

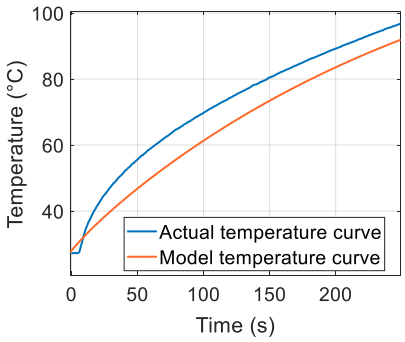

Fig.5 Actual temperature and model temperature curves

4.2 Simulation results

Simulation is performed on the established model of the controlled object to construct an adaptive neural network controller system, which is then validated through simulation experiments. Initially, the algorithm demonstrates the ability to automatically track input signals without the need for a system model. Subsequently, the robustness of the system is assessed by introducing disturbance signals.

4.2.1 The signal tracking performance test

Parameters obtained from the signal following the test and the input signal (Eq. 52) are selected to simulate the output of RBFNN based on the Nussbaum-type function:

$$\begin{cases} x_{in}(t) = 0.6 * t & t \in [0, 83] \\ x_{in}(t) = 50 & t > 83 \end{cases}, \quad (52)$$

The adaptive rate parameters of Eqs. (36) and (37) are $\sigma = 0, \rho = 0, k_1 = 1$, $\mathrm{k}_2 = 1$, $r_1 = -20$, and $r_2 = -10$, and the initial value of the integrator is - 5. The neural network parameters in Eq. (3) are $\mu_i = [0, -1, -0.5, 0, 0.5, 1]^T$.

In addition, a PID controller for the same object was designed for comparison. Parameters of the PID controller are adjusted as $\mathrm{P} = 100, \mathrm{I} = 10, \text{and } \mathrm{D} = 0$ to obtain a similar effect with the RBFNN controller. The following effect obtained from these two controllers is shown in Fig. 6:

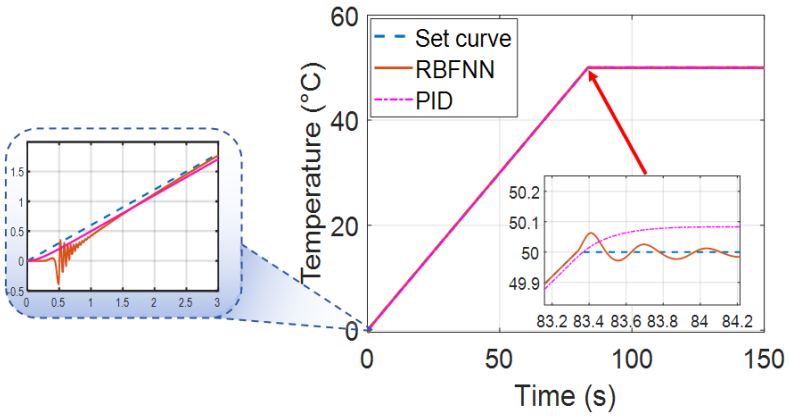

Fig.6 Signal-following curves of two controllers without interference

The results (as shown in Fig. 6) indicate that in the initial phase, under the dual influence of the RBF neural network and the Nussbaum function, the controller is capable of automatically adjusting and progressively identifying the model of the controlled object. After 1.5 seconds, the system output converges and tracks the pre-set temperature curve. Compared with the PID curve, the neural network parameters are fixed, indicating the range of neural network adjustment. In contrast, the PID parameters are a set of optimal parameters selected through empirical tuning. The experimental results demonstrate that after automatic adjustment, the tracking performance of the neural network is comparable to that of the PID. After the neural network structure stabilizes, it exhibits higher steady-state accuracy and better stability when the signal changes. This achieves control effects without the need for manual modeling and repeated PID parameter adjustments, simplifying the parameter tuning process.

4.2.2 Robustness test of the control algorithm

A disturbance signal with a value of ±5°Cs introduced into the controlled object. Since most disturbances in the system are slowly changed disturbance signals, the disturbance signal is filtered by the first-order inertia link with k = 1 and t = 1. The output of the two controllers in the presence of disturbance is shown in Fig. 7.

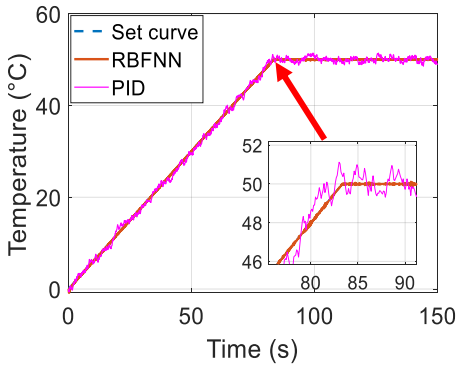

Fig. 7. Signal-following curves of two controllers under random disturbance

Compared with the signal-following curve before and after adding disturbance, the new RBFNN controller based on the Nussbaum-type function has a stronger anti-interference ability than the traditional PID controller and a strong inhibition effect on the slowly changed disturbance signal.

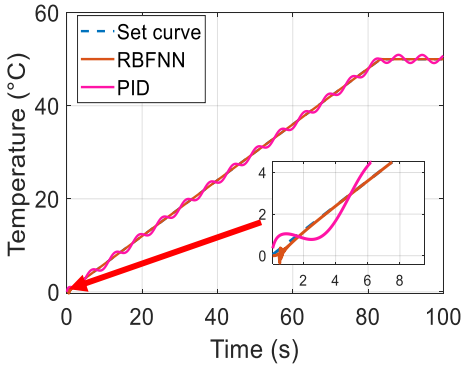

Fig. 8. Signal-following curves of two controllers under sinusoidal disturbance

The sinusoidal disturbance is another type often encountered by the extruder machine system. Thus, it is necessary to test these two controllers under sinusoidal disturbance input. Here, a periodic disturbance signal with an amplitude of 5 °C and a period of 1 rad/s is added to the system. The output signal of PID and RBFNN controllers are shown in Fig.8. The results show that the output of the RBFNN controller quickly tends to stabilize after the adjustment in the initial stage. However, the PID controller has a limited ability to suppress sinusoidal disturbance. Therefore, the RBFNN controller is characterized by a stronger anti-interference ability than the PID controller. The main purpose of the RBFNN controller is more suitable for industrial applications, where sinusoidal interference is severe.

5. Findings and results

Through algorithm design and experimental simulation verification, we have obtained a design method based on a neural network controller. This algorithm has the following advantages compared to traditional PID algorithms:

1. It possesses the advantage of participating in fixed parameter inputs, eliminating the need for specialized parameter tuning for specific performance equipment, thus reducing the difficulty of manual PID parameter adjustment.

2. The system exhibits stronger robustness when subjected to random disturbances (simulating the impact of room temperature changes on an injection molding machine) and sinusoidal disturbances (simulating the impact of power grid noise on the system), demonstrating superior performance.

6. Conclusions

This paper proposes an adaptive temperature control algorithm based on Radial Basis Function Neural Network (RBFNN) and Nussbaum-type function. Utilizing the nonlinear fitting characteristics of RBFNN, the algorithm achieves automatic modeling of the extruder's temperature. The designed controller addresses the issues of low temperature control precision, difficult parameter selection, and poor robustness in extruder design. The problem of the unknown coefficient direction of the controller's 'u' is resolved using a Nussbaum-type function. Simulation results indicate that compared to traditional PID control algorithms, the proposed algorithm can accurately follow the input temperature and possesses strong anti-interference capabilities. If this algorithm could be implanted into the actual extruder system, it would significantly enhance the ability to resist temperature disturbances during steady-state operation.

There is still some distance from practical application, mainly because: no actual system can be an energy-unlimited system, system inputs are constrained, and the problem of designing controller outputs under nonlinear constraints still needs further research. Additionally, actual control systems are discrete, and subsequent work will further study the discretization of continuous systems. Methods based on event-triggering have already begun experiments and have made certain progress.

Moreover, this algorithm can also be applied to other nonlinear systems with large inertia that are subject to disturbances, especially in equipment requiring precise temperature control, such as sintering furnace temperature control used in solar cell production and temperature management in wafer-level bonding and debonding equipment in semiconductor manufacturing. This highlights its importance in practical engineering applications.

Acknowledgment

This research is part of a special project for the construction of the Beijing Tianjin Hebei collaborative innovation community: "Research and application of key technologies of wafer transfer robot in a clean environment" (22341802D).

This research is funded by the Young Backbone Teacher Support Plan of Beijing Information Science &Technology University (YBT 202401).

This research is funded by "Beijing Changping District Deputy Chief Technology Officer Project".

R E F E R E N C E S

[1]. *Cao YP, Ming WD, Long WB, Liu HJ, Zhang L.* "Effects of Process Condition on Stability of Output in Single Screw Extruding Procedure". Plastics. **vol. 30**, no. 3, 2001, pp. 46-48

[2]. *Traintinger M, Kerschbaumer RC, Lechner B, Friesenbichler W, Lucyshyn T.* "Temperature Profile in Rubber Injection Molding: Application of a Recently Developed Testing Method to Improve the Process Simulation and Calculation of Curing Kinetics". Polymers, **vol. 13**, no. 3, 2021, pp. 1-12.

[3]. *Guo J, Bao J, Zhu J, Zheng T, Zhou W.* "Intelligent temperature control research of injection device in low pressure injection molding machine". Industrial Instrumentation & Automation, no.6, 2016, pp.27-30.

[4] *Mehdi M, Chalak Q M R, Vahid P*."Optimized injection-molding process for thin-walled polypropylene part using genetic programming and interior point solver". The International Journal of Advanced Manufacturing Technology, no.124, 2023, pp.297 – 313.

[5]. *Dormeier S.* Extruder Control. IFAC Proceedings Volumes.no.13, 1980, pp.551-60.

[6]. *Dastych, J., P. Wiemer, and H. Unbehauen.* "Robust and Adaptive Control of a Single Screw Plastics Extruder." IFAC Proceedings., **vol.21,** no.7, 1988, pp.171-176.

[7]. *Liang CC, Feng XY, Qiang LV, Zheng J.* "Temperature Control System of Masterbatch Production Line Based on Fuzzy Adaptive PID", Modular Machine Tool & Automatic Manufacturing Technique. no.4, ,2017, pp. 96-98.

[8]. *Yao K, Gao F.* "Optimal start-up control of injection molding barrel temperature", Polymer Engineering & Science., no.47, 2007, pp. 254–261.

[9]. *Se-Kyu, et al.* "Iterative learning model predictive control for constrained multivariable control of batch processes.", Computers & Chemical Engineering: An International Journal of Computer Applications in Chemical Engineering, no.93,2016, pp.284-292.

[10]. *Wen, S. P., Jiang, J., Qu, J. P., & Jin, G.* (2010). "Multivariable fuzzy decoupling control of the polymer electromagnetism dynamic extrusion process.", Journal of applied polymer science, **vol.116,** no.1, pp.568-576.

[11]. *Peng Y, Wei W.* "Melt temperature dynamic control strategy of injection molding machine based on variable structure control and iterative learning control". Journal of Polymer Engineering, **vol.31,** no.7, 2011, pp.473-478.

[12]. *Peng Y, Wei W.* "Melt temperature learning control of injection molding process based on CMAC neural network". Journal of Polymer Engineering, **vol.31,** no.1, 2011, pp.45-52.

[13]. *Yanan Hu, Hongxing Z, Huiping F, et al.* "Temperature Control Strategy of Injection Molding Machine Barrel Based on Fuzzy Neural Network". Plastics, **vol.4,** no.2, 2019, pp.18-25.

[14] *Lin F, Duan J, Lu Q.* "Optimization Of In Injection Moding Quality Based On BP Neural Network And PSO". Materiali in Tehnologije, **vol.3,** no.12, 2022, pp.28-38.

[15] *Lai W J, Chen S.* "The Control Research of Neural Network on Barrel Temperature of The Plastic Injection-Molding Machine". Applied Mechanics and Materials, **vol.9,** no.2, 2011, pp.52-54.

[16]. *Zhu H.* "Application of Single Neuron Adaptive PID Control Based on RBF in Single Screw Extruder", Journal of Huangshi Institute of Technology., **vol.26,** no.1, 2010. pp. 5-8.

[17]. *Lai W J, Chen S.* "The Control Research of Neural Network on Barrel Temperature of The Plastic Injection-Molding Machine", Applied Mechanics and Materials, no. 52, 2011, pp. 1656-1659.

[18] *Xu Y, Zhang Y, Zhang J F.* "Singularity-free adaptive control of discrete-time linear systems without prior knowledge of the high-frequency gain". Automatica, **vol.17,** no.1, 2024, pp.165-173.

[19] *Yan K , Chen C , Xu X ,et al.* "Neural Network-Based Output Feedback Fault Tolerant Tracking Control for Nonlinear Systems with Unknown Control Directions". Complexity, **vol.11,** no.2, 2022, pp.12-22.

[20]. *Oliveira TR, Peixoto AJ,* Nunes E. "Binary robust adaptive control with monitoring functions for systems under unknown high-frequency-gain sign, parametric uncertainties and unmodeled dynamics", International Journal of Adaptive Control & Signal Processing., no. 30,2016, pp. 1184-202.

[21]. *Bounemeur, A., and M. Chemachema.* "General fuzzy adaptive fault-tolerant control based on Nussbaum-type function with additive and multiplicative sensor and state-dependent actuator faults", Fuzzy sets and systems, **vol. 468,** no.108616, 2023, pp. 1-27.